

# Acoustic-Laser Vibrometry for Standoff Detection of Defects in Materials

Oral BUYUKOZTURK <sup>1</sup>, Justin G. CHEN <sup>1</sup>, Timothy J. EMGE II <sup>1,2</sup>, Robert W. HAUPT <sup>3</sup>

<sup>1</sup> Department of Civil and Environmental Engineering, Massachusetts Institute of Technology  
Cambridge, MA, USA, Phone: +1 617 253 7186;  
e-mail: obuyuk@mit.edu, ju21743@mit.edu, tim.emge2@gmail.com

<sup>2</sup>U.S. Navy, Norfolk, VA, USA

<sup>3</sup> MIT Lincoln Laboratory; Lexington, MA, USA; e-mail: haupt@ll.mit.edu

## Abstract

Standoff methods of non-destructive testing (NDT) offer flexibility over traditional methods of inspection which typically require physical contact with the material being measured. The benefits are that difficult to access locations can be inspected and measurements of a large area can be made more quickly. Acoustic-laser vibrometry is a robust standoff NDT technique for composite materials, specifically implemented on fiber reinforced polymer (FRP) strengthened concrete and steel composites. The technique exploits differing responses in intact and defective interfaces between material layers from mechanical effects. An acoustic wave excites the composite system and causes it to vibrate; defects such as voids and delaminations will vibrate excessively like a drum head, which are measured and identified by the laser vibrometer. In this paper first fundamentals of acoustic-laser vibrometry and its underlying technologies will be provided, followed by description and discussion of measurements on FRP-concrete and FRP-steel laboratory specimens. Issues regarding the inspection of materials and parameters specific to standoff measurement such as defect size, distance, angle of incidence, and probability of detection will be discussed.

**Keywords:** Civil engineering, acoustic-laser vibrometry, non-contact, interface defects, FRP-concrete, steel composites

## 1. Introduction

### 1.1 Background

Traditional non-destructive testing (NDT) methodologies involve easy access to the material being evaluated as physical contact or visual inspection is necessary. Non-contact or standoff methods where measurements can be made from a distance are advantageous in situations where such access is not available, allowing for a wider range of structures to be inspected. Non-contact methods acquire information from materials under test through waves that are electromagnetically or acoustically propagated. Many standoff techniques make use of lasers using their mono-chromatic nature for measurements of an interferometric nature. Laser vibrometry uses the Doppler shift induced on a carrier frequency of the laser by a moving surface to measure the velocity of that surface [1]. This allows for highly accurate measurements of the velocity of a surface, which with the correct experimental setup can be used to evaluate physical properties of materials.

### 1.2 Purpose

Acoustic-laser vibrometry makes use of an airborne acoustic excitation to vibrate a material and a laser vibrometer to measure the vibrational frequency response to determine the physical characteristics of a composite material. The marked difference in the response will identify materials as either intact or defective. Previous work showed that acoustic-laser vibrometry was capable of detecting anomalies in the ground due to the presence of land mines, so the method was adapted for NDT of structures [2]. This paper will describe the application of the acoustic-laser vibrometry method to non-contact NDT of composite

materials, specifically fiber reinforced polymer (FRP) strengthened concrete and steel composites, the validity of which was previously demonstrated [3, 4]. The focus of this paper will be on the phenomenology of the method along with the effects of different parameters and their relation to real world measurements. The methodology and theory behind the method will be presented with representative measurements on test specimens measured with a laboratory system. The probability of detection of the system as a result of those measurements will be discussed along with parameters influencing the measured defect signals including defect size, distance, and angle of incidence.

## 2. Methodology and Theory

### 2.1 Concept

As previously described, the acoustic-laser vibrometry method involves an airborne acoustic excitation and a laser vibrometer for vibration measurement. The method was developed specifically for the inspection of composite materials where multiple layers of material are bonded together by an adhesive or epoxy. When properly bonded the material vibrates little due to the acoustic excitation, but when there are delamination defects or voids under the covering materials, the top layer of material will vibrate in excess of the surrounding properly bonded material like a drum head. The laser vibrometer measures the velocity of the surface of the material, looking for areas where the amplitude is excessive. This is illustrated in Figure 1 on FRP-concrete material, but the concept is the same for any other composite material.

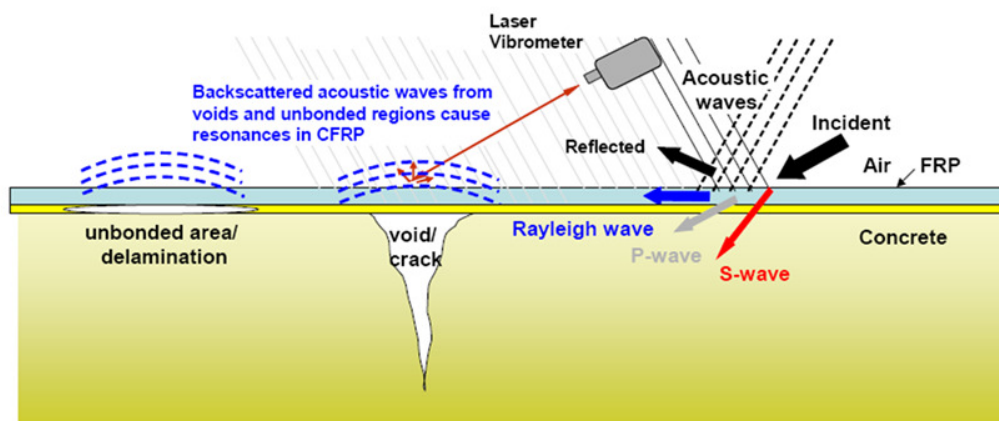


Figure 1. Illustration of the acoustic-laser vibrometry method [3]

The acoustic excitation used typically consists of a broadband signal that excites the defect at a wide range of frequencies. Either white noise or frequency sweep tones are used which excite the defect at its resonant frequencies. Once the laser vibrometer measures the vibration of a defective region, the signal can be transformed into the frequency domain to obtain the resonant frequency response of the defect. The specific resonant frequencies of the defect can reveal characteristics of the defect such as the size or aspect ratio as long as material properties are known for the material.

### 2.2 Theory

A defect, either delamination or void, can be represented by a clamped plate as a simplified model. The regions where the material is intact are not considered and the clamped boundary is the boundary of the defect where the debonded area starts. For simplicity, a square defect is

considered and a diagram of the model is shown in Figure 2. The resonant frequency  $f$  for this clamped plate are determined by Equation 1, where  $D$  is the flexural rigidity defined in Equation 2,  $E$  = Young's modulus,  $h$  = thickness of the plate,  $\nu$  = Poisson's ratio of the material,  $\rho$  = density of the material,  $a$  = side length of the square plate, and  $\lambda$  = a frequency parameter that depends on the resonant mode, geometry, and boundary conditions of the plate [5].

$$f = \frac{\lambda}{2\pi a^2} \sqrt{\frac{D}{\rho h}} \dots\dots\dots (1)$$

$$D = \frac{Eh^3}{12(1-\nu^2)} \dots\dots\dots (2)$$

The expected resonant frequencies of the different vibrational modes of the model plate can be calculated. Resonant frequencies were calculated from material properties for FRP and dimensions from the defect on the FRP-concrete specimen, shown in Table 1. These material properties are not measured numbers from our specific FRP-concrete specimen, and can only be treated as approximate. This model also considers FRP an isotropic material, despite FRP being highly directional. When measuring defects, if the precise materials properties of the FRP or other target material are known, the inverse problem of determining the defect size from the measured resonance frequencies can be solved given a certain geometry and boundary condition. In general, larger defects in thinner materials will have lower resonant frequencies, and smaller defects in thicker materials will have higher resonant frequencies.

**Table 1. Material properties and estimated resonant frequencies**

Material Properties of FRP		Calculated Resonant Frequencies	
Defect side length	0.0381 m	Mode	Frequency (Hz)
Young's modulus	20.9 GPa	1, 1	5151
Poisson's ratio	0.2	2, 1	10503
Density	1800 kg/m <sup>3</sup>	2, 2	15488
Thickness	1.3 mm	3, 1	18875

**2.3 Experimental Methods**

*2.3.1 Measurement Procedure*

The test system consists of a commercial laser vibrometer, desktop speaker for acoustic excitation, microphone to measure the sound pressure level (SPL) at the specimen, and data collection equipment. The specimen is located approximately 2 meters from the laser vibrometer and has a small spot of retroreflective tape for optimal laser return signal. The speaker is located 1 meter from the specimen and placed off the line of sight of the laser vibrometer. The basic measurement consists of using the speaker to play a frequency sweep sound with a bandwidth of 0 Hz to 20 kHz and a duration of 60 seconds to excite the test specimen. During this excitation, the laser vibrometer and microphone are measuring the velocity of the surface of the specimen and the sound received at the specimen respectively. The velocity time series measured by the laser vibrometer is processed with a fast Fourier transform (FFT) to obtain the frequency velocity response of the specimen in the measured location. The amplitudes are also scaled by a factor of the square root of the frequency sweep duration multiplied by the bandwidth so that the amplitude would be similar to that obtained with a single frequency excitation. This allows for easy visualization of the resonant frequencies of the defects.

### 2.3.2 Experimental Specimens

Two different types of experimental specimens are used in this paper to demonstrate the flexibility of the acoustic-laser vibrometry method on different types of composite materials. The first specimen is FRP-concrete that consists of a concrete panel that is 30.5 cm by 30.5 cm by 10.2 cm and an approximately 1.3mm thick FRP laminate covering, with a defect that consists of a 3.8 cm by 3.8 cm by 2.5 cm deep void in the concrete, shown in Figure 2a, which was the basis for the resonant frequency calculation in Table 1. The second specimen is a FRP-steel composite consisting of a 9.5 mm thick steel plate with a much thicker 4.8 mm FRP laminate, and an elliptical debond defect with major and minor axes of 11.4 cm and 8.9 cm, shown in Figure 2b [4].

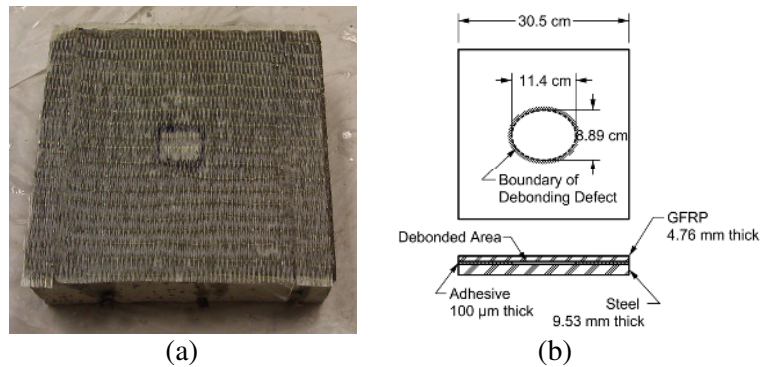


Figure 2. (a) FRP- concrete specimen and (b) FRP-steel specimen [4]

## 3. Results

### 3.1 FRP-concrete Specimen

Measurements were made on the defect of the FRP-concrete specimen and over an area of intact material as shown in Figures 3a and 3b respectively. A resonant peak for the defect was found at 3200 Hz with an amplitude of almost 3000  $\mu\text{m/s}$  compared to the measurement of the intact material which has no resonance peak and a noise floor of 20  $\mu\text{m/s}$ . This gives a potential signal to noise ratio (SNR) of well over 100 and well identifies the defective area on this specimen.

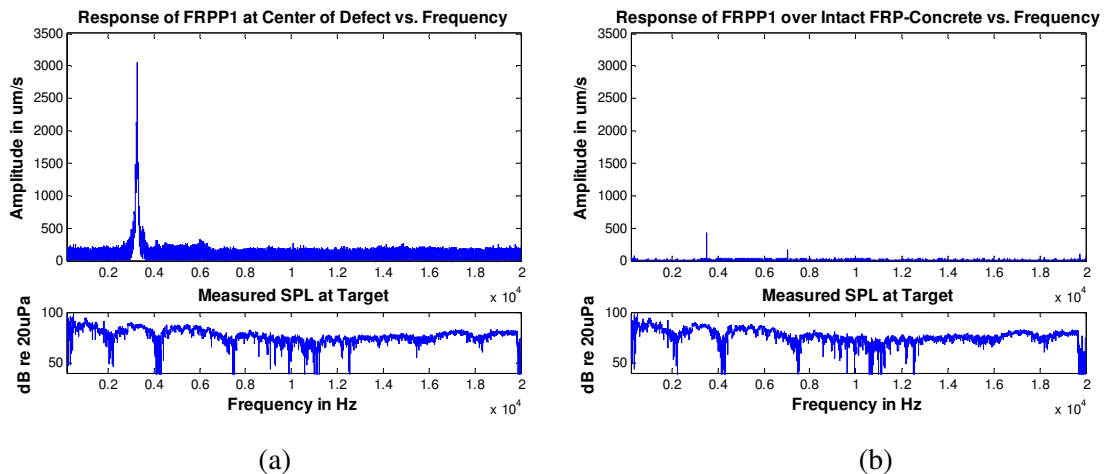


Figure 3. Measurement results for FRP-concrete specimen over (a) the defect and (b) intact material

To obtain an image of the vibration velocity of the whole defect a set of measurements in a 13 by 10 grid with 0.5 cm spacing were made over an area including the defect and the surrounding intact material, using a 10 second 0 Hz - 20 kHz frequency sweep excitation for each measurement. The results are shown in Figure 4, showing the first three resonant modes with clearly visible modal behavior.

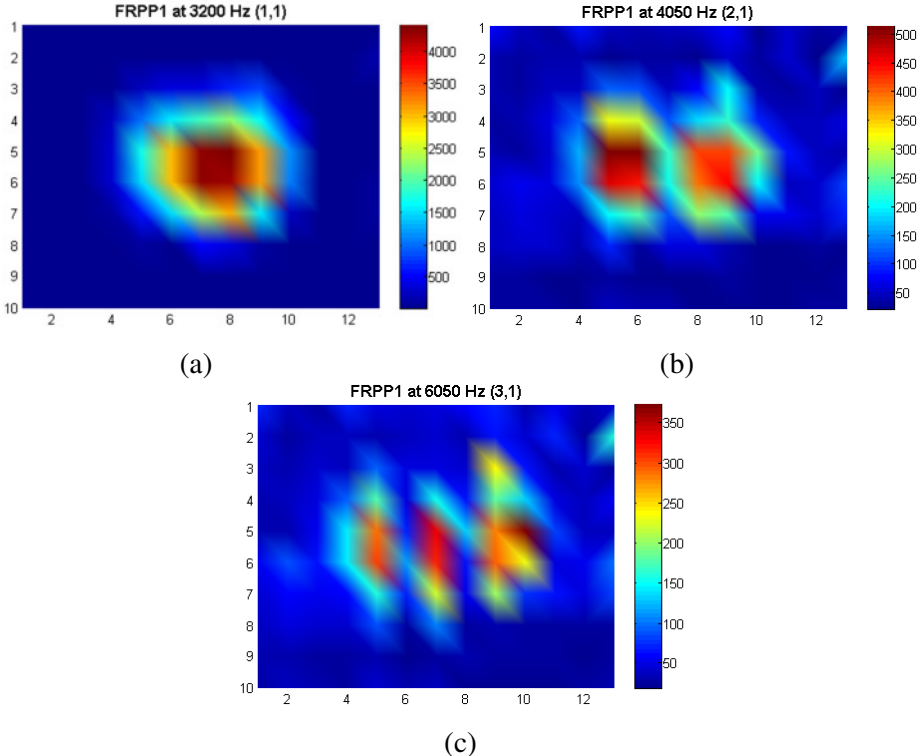


Figure 4. Imaging of the FRP-concrete defect at (a) 3200 Hz, (b) 4050 Hz, and (c) 6050 Hz

From the series of measurements made, a receiver operating characteristic (ROC) curve can be calculated which relates the true positive rate to the false positive rate and is a measure of the system performance [6]. A velocity is chosen as the boundary between a detection of a defect and intact material, and the true and false positive rates are calculated accordingly. The result is shown in Figure 5, and the system achieves a 90% positive detection rate with a 2.3% false positive rate.

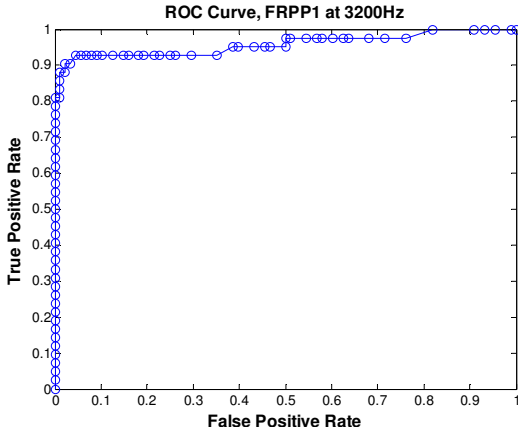


Figure 5. ROC curve calculated from 3200 Hz measurement of FRP-concrete specimen

**3.2 FRP-steel Specimen**

The measurements made on the FRP-steel specimen are shown in Figure 6, with the defect exhibiting a vibration velocity of  $170 \mu\text{m/s}$  at  $2535 \text{ Hz}$  compared to an intact area of the material with a velocity of  $20 \mu\text{m/s}$  [4]. The sharp peaks seen in both plots are likely due to noise and do not correspond to any physical resonances of the measured specimen.

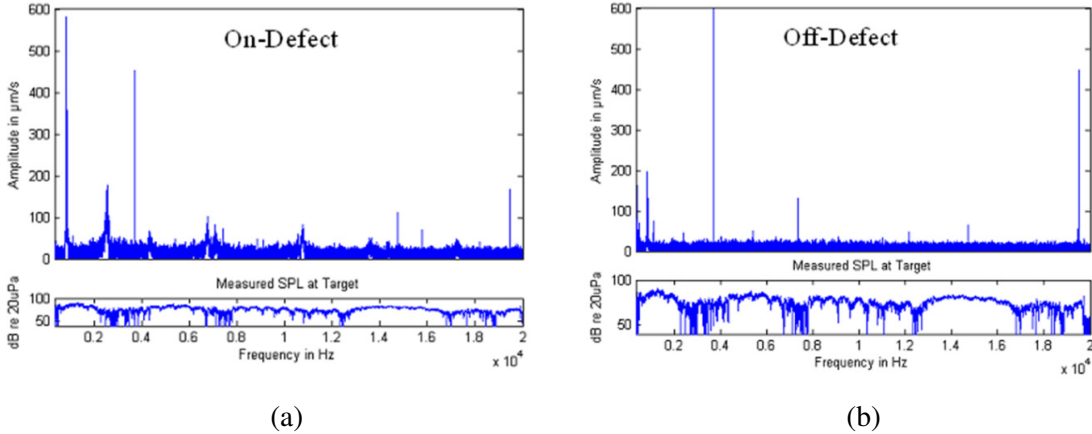


Figure 6. Measurement results for FRP-steel specimen over (a) the defect and (b) intact material

To image the vibration velocity of the FRP-steel specimen measurements were made in a 7 by 9 grid over the defect with an approximate spacing of  $1.5 \text{ cm}$  [4]. The result shown in Figure 7a for at  $2535 \text{ Hz}$  shows the first resonant mode of the defect and the surrounding intact region with a much lower vibration velocity. The ROC curve calculated from this measurement is shown in Figure 7b and the system achieves a  $75.93\%$  positive detection rate with a  $0\%$  false positive rate.

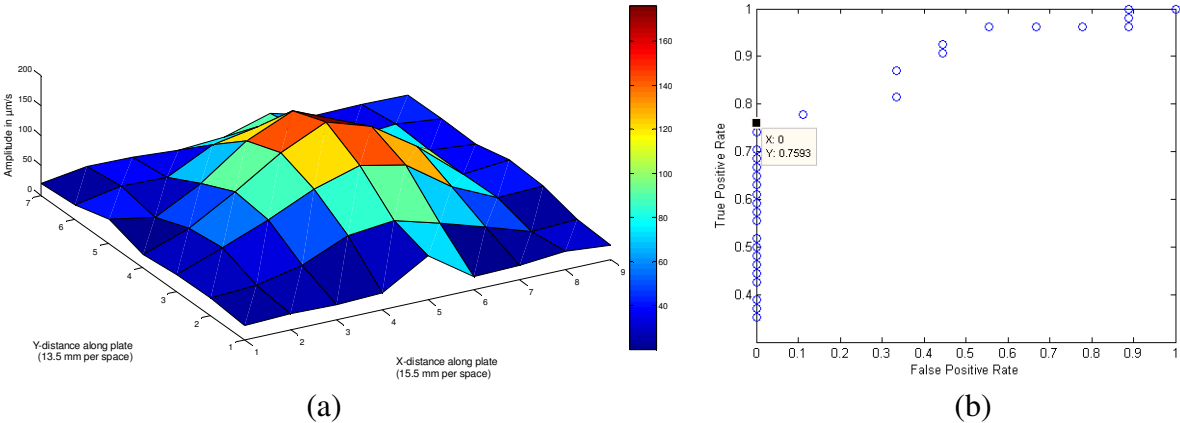


Figure 7. (a) Image of the FRP-steel specimen at  $2535 \text{ Hz}$  and (b) ROC curve calculated from the same measurement

### 3.3 Parametric Studies

Several parameters were tested for their effect on system measurements, either the measured defect vibration amplitude, the noise floor, or both, characterized by the SNR. The important parameters to consider in real-world measurements are the distance, angle of incident to the target surface, and dwell time or measurement duration. There are two possible distances to consider, the distance of the acoustic excitation affecting the sound pressure level (SPL), and the distance of the laser vibrometer affecting the laser signal reflected back from the target.

### 3.3.1 Sound Pressure Level

The SPL will decrease as a function of distance from the acoustic source as shown in Figure 8a. The effect of a lower SPL is that less energy is available to vibrate the defect at the surface of the material being measured. The result of varying SPL on a measurement of the FRP-concrete specimen is shown in Figure 8b where a single sine wave tone with a duration of 60 was used as the excitation. With an increase of 20 dB of the SPL, the vibration amplitude of the defect increased by a factor of 10.

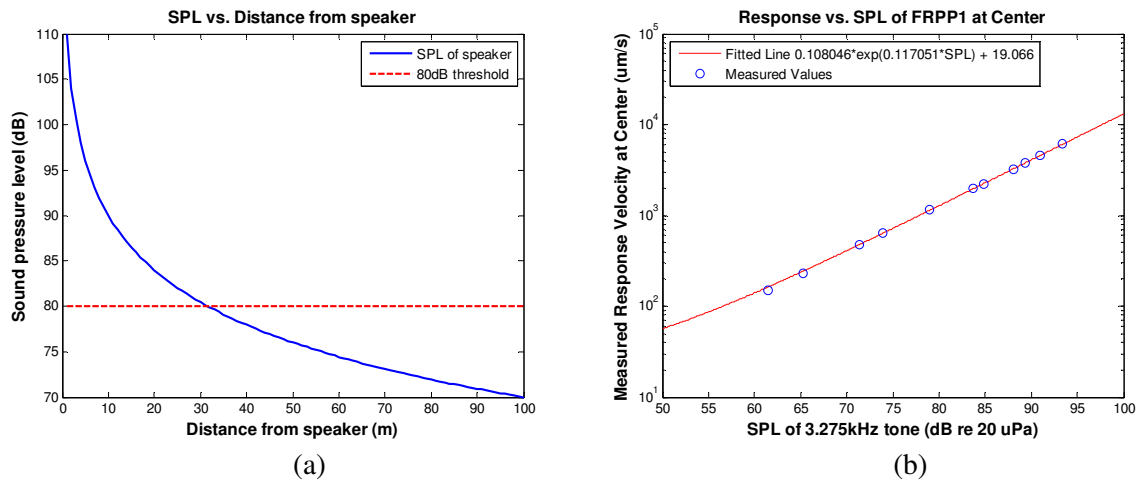


Figure 8. (a) SPL as a function of speaker distance and (b) Effect of SPL on defect vibration amplitude

### 3.3.2 Laser Signal

To simulate the effect of the laser vibrometer being further away from the target, neutral density filters were used to reduce the output light and the received light reflected back from the target. The result when measuring the FRP-concrete specimen shown in Figure 9 is that a reduction in the reflected light received corresponds directly to an increase in the noise floor. The vibration amplitude of these measurements did not vary, so the effect is confined to the sensor noise floor.

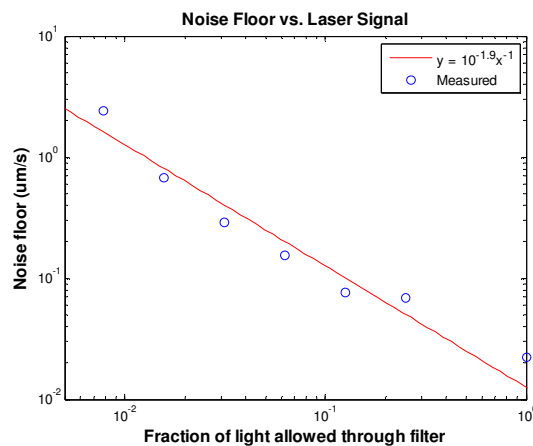


Figure 9. Effect of laser signal or simulated distance on the measurement noise floor

### 3.3.3 Angle of Incidence

The angle of incidence of a measurement is especially relevant since the materials be measured are expected to be in difficult to reach areas. In this set of measurements both the angle of the acoustic excitation and the laser vibrometer were varied. The results for the FRP-concrete and FRP-steel are shown in Figure 10. The FRP-concrete results in Figure 10a are indeterminate due to the rippling of the FRP-surface with a surface roughness greater than the size of the laser vibrometer spot. This effect changes the true angle of incidence of the laser vibrometer and could possibly be used as an advantage for measuring surfaces at an oblique angle as long as the acoustic excitation is loud enough to excite the defect. On the FRP-steel specimen in Figure 10b we see an expected cosine squared effect, with the angle of the acoustic excitation and the laser vibrometer each having a cosine dependence [4].

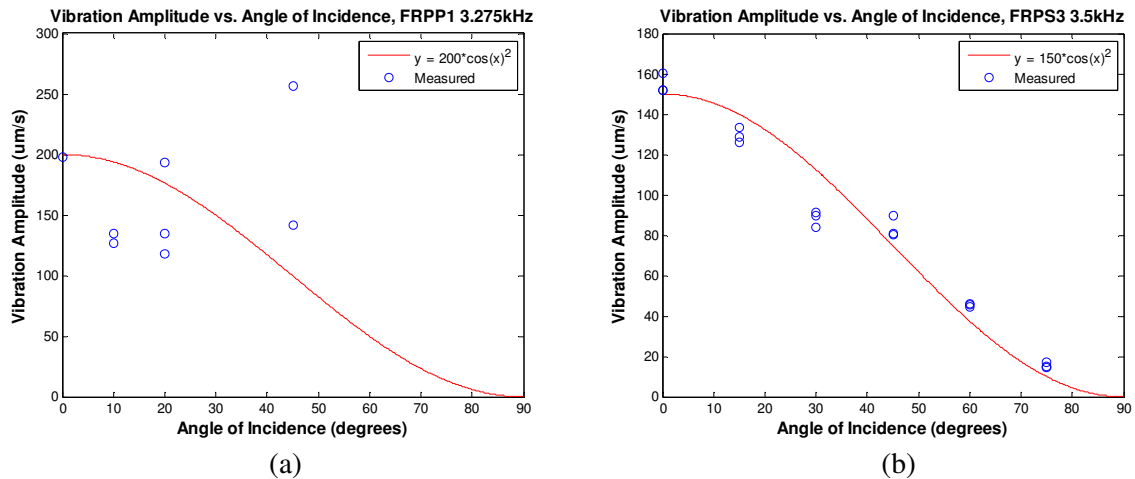


Figure 10. Angle of incidence measurement results on (a) FRP-concrete and (b) FRP-steel

### 3.3.1 Dwell Time

The effect of the measurement dwell time for both a single tone sine wave excitation at the defect resonant frequency and broadband white noise excitation was tested on the FRP-concrete specimen, with the results shown in Figure 11. In the case of the sine wave excitation in Figure 11a the SNR improves directly as the dwell time increases, however with the white noise in figure 11b the SNR improves only by a factor of 10 as the dwell time increases by a factor of 1000.

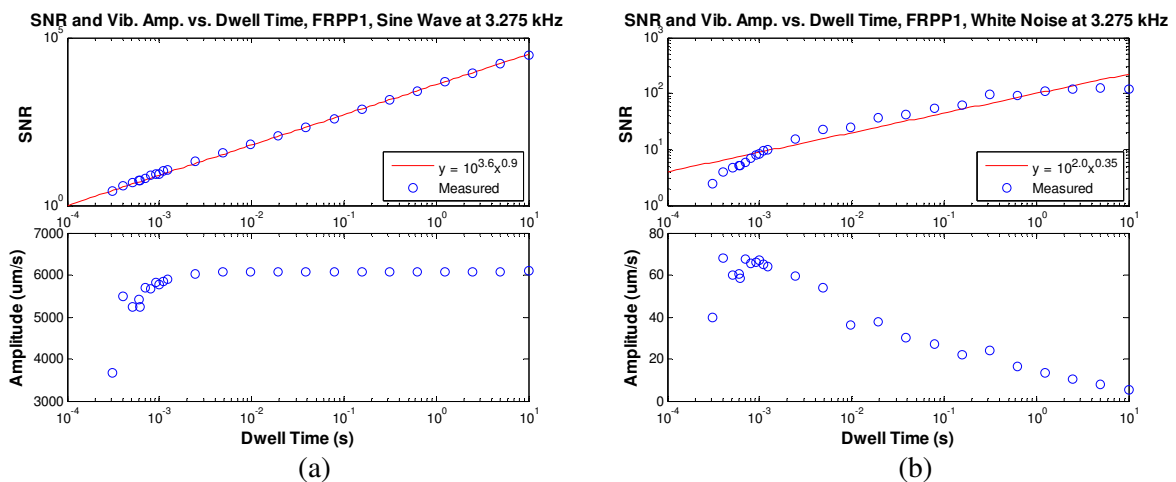


Figure 11. Effect of dwell time on SNR with acoustic excitation of (a) sine wave and (b) white noise



Despite there being a great effect due to the measurement duration for a sine wave and white noise excitation, a similar study was carried out for a frequency sweep acoustic excitation with sweep durations of 0.1, 1, 10, and 60 seconds, measured on the FRP-concrete specimen. The SNR does not appreciably change with these different sweep durations, with the rest of the results summarized in Table 2. The SNR is similar to what is achieved with a white noise excitation with a dwell time of only 1 ms, suggesting that the current processing scheme for a frequency sweep measurement could be improved.

**Table 2. Results from frequency sweep duration study**

Sweep Duration	Frequency	Average SPL	Amplitude	Noise Floor	SNR
0.1 seconds	3247.8 Hz	80.3481 dB	5068.0 $\mu\text{m/s}$	74.0646 $\mu\text{m/s}$	68.4268
1 second	3245.7 Hz	80.4217 dB	4909.4 $\mu\text{m/s}$	74.6392 $\mu\text{m/s}$	65.7751
10 seconds	3246.6 Hz	80.4584 dB	4972.1 $\mu\text{m/s}$	73.1881 $\mu\text{m/s}$	67.9359
60 seconds	3247.0 Hz	80.2238 dB	5097.8 $\mu\text{m/s}$	73.5018 $\mu\text{m/s}$	69.3561

#### 4. Conclusion

The acoustic-laser vibrometry method has been shown to identify defective areas of composite materials in a non-contact manner based on changes in physical properties. The acoustic source excites the target material while the laser vibrometer measures a velocity time series. The defect, which may consist of a delaminated area or void underneath the covering material, will vibrate in excess of the surrounding intact material. It will vibrate with resonant frequencies that can be determined by modelling the defect as a clamped plate. Measurements were made of FRP-strengthened concrete and FRP-steel composite specimens to demonstrate the method and determine the effects of different system parameters on defect detectability.

Defects in the FRP-strengthened concrete specimen and FRP-steel composite specimen were measured and detected with SNRs of 100 and 8 respectively. A grid of measurements over the defect surface were used to generate images of the vibration amplitude showing the resonant modes and the defect boundaries. Based on these measurements the system achieved a 90% positive detection rate with a 2.3% false positive rate on the FRP-concrete specimen and a 75.9% positive detection rate with a 0% false positive rate on the FRP-steel specimen. An increase of 20 dB in the SPL increases the vibration amplitude of the defect by a factor of 10. A simulated doubling of the distance of the laser vibrometer from the target reduced the laser signal level or amount of light received by the laser vibrometer by a factor of 4 and increased the noise floor by a factor of 4. The angle of incidence of the acoustic source controls the defect vibration amplitude directly with a cosine factor and the angle of incidence of the laser vibrometer alters the measured velocity also by a cosine factor. The measurement dwell time for a constant tone sine wave acoustic excitation is directly proportional to the SNR, and for a white noise excitation the SNR improves proportional to the cube root of the dwell time. With a frequency sweep acoustic excitation, for a bandwidth of 0-20 kHz and durations of 0.1 seconds to 60 seconds, the SNR is unchanged.

Detectability of a defect when measured by the acoustic-laser vibrometry method is dependent on clearly distinguishing the defect vibration velocity from the noise floor of the velocity measurement, which can also be defined as the SNR. Defects will vibrate with different amplitudes depending on their size and thickness with thinner, larger defects vibrating with greater amplitude given the same acoustic excitation. For example, similar strength acoustic excitations vibrate the 1.3 mm FRP concrete cover 20 times that of the 4.8

mm thick FRP on the FRP-steel specimen. Increasing the SPL of the acoustic excitation will increase the defect vibration amplitude, however there will be a limit to the loudness available from acoustic sources. Distance is a detrimental effect to the SNR in that it not only decreases the SPL, but also increases the noise floor of the measurement. Measurement times depending on the excitation will also impact the SNR. A field acoustic-laser vibrometry system will need to balance distance and defect detectability, and capabilities will change for different material types.

### **Acknowledgements**

The authors acknowledge the support provided by the National Science Foundation (NSF) under CMMI Grant No. 0926671. MIT Lincoln Laboratory provided the experimental equipment and facilities. Naval Surface Warfare Center, Carderock Division donated the composite and steel plates used for the FRP-steel specimen. At the time of this work, Justin Chen was supported by Royal Dutch Shell through the MIT Energy Initiative. Finally, we express our appreciation of the American Society for Nondestructive Testing (ASNT) for their support through the 2011 Fellowship Award to Professor O. Buyukozturk and graduate student J. Chen.

### **References**

1. A L Kachelmyer and K I Schultz, 'Laser vibration sensing', Lincoln Laboratory Journal, Vol 8, No 1, pp 3-28, 1995.
2. R Haupt and K D Rolt, 'Stand-off acoustic-laser technique to locate buried landmines', Lincoln Laboratory Journal, Vol 15, No 1, pp 3-22, 2004.
3. O Buyukozturk, R Haupt, C Tuakta, and J Chen, 'Remote detection of debonding in FRP-strengthened concrete structures using acoustic-laser technique', Nondestructive Testing of Materials and Structures, RILEM Bookseries 6, O Buyukozturk et al. eds, Springer, pp 19-24, 2013.
4. T Emge and O Buyukozturk, 'Remote nondestructive testing of composite-steel interface by acoustic laser vibrometry', Materials Evaluation, Vol 70, No 12, pp 1401 - 1410, 2012.
5. A W Leissa, Vibration of Plates, SP-160, NASA, US Government Printing Office, Washington, D.C, 1969.
6. T Fawcett, 'An introduction to ROC analysis', Pattern Recognition Letters, Vol 27, Iss 8, pp 861-874, 2006.